

REPORT DOCUMENTATION PAGE			Form Approved OMB NO. 0704-0188		
<p>The public reporting burden for this collection of information is estimated to average 1 hour per response, including the time for reviewing instructions, searching existing data sources, gathering and maintaining the data needed, and completing and reviewing the collection of information. Send comments regarding this burden estimate or any other aspect of this collection of information, including suggestions for reducing this burden, to Washington Headquarters Services, Directorate for Information Operations and Reports, 1215 Jefferson Davis Highway, Suite 1204, Arlington VA, 22202-4302. Respondents should be aware that notwithstanding any other provision of law, no person shall be subject to any penalty for failing to comply with a collection of information if it does not display a currently valid OMB control number.</p> <p>PLEASE DO NOT RETURN YOUR FORM TO THE ABOVE ADDRESS.</p>					
1. REPORT DATE (DD-MM-YYYY) 05-01-2020		2. REPORT TYPE Final Report		3. DATES COVERED (From - To) 6-Apr-2016 - 5-Oct-2019	
4. TITLE AND SUBTITLE Final Report: Novel metamorphic heterostructures for long wave infrared optoelectronics			5a. CONTRACT NUMBER W911NF-16-2-0053		
			5b. GRANT NUMBER		
			5c. PROGRAM ELEMENT NUMBER 611102		
6. AUTHORS			5d. PROJECT NUMBER		
			5e. TASK NUMBER		
			5f. WORK UNIT NUMBER		
7. PERFORMING ORGANIZATION NAMES AND ADDRESSES Research Foundation of SUNY at Stony Brc W-5510 Melville Library Stony Brook, NY 11794 -3362			8. PERFORMING ORGANIZATION REPORT NUMBER		
9. SPONSORING/MONITORING AGENCY NAME(S) AND ADDRESS (ES) U.S. Army Research Office P.O. Box 12211 Research Triangle Park, NC 27709-2211			10. SPONSOR/MONITOR'S ACRONYM(S) ARO		
			11. SPONSOR/MONITOR'S REPORT NUMBER(S) 68326-EL.19		
12. DISTRIBUTION AVAILABILITY STATEMENT Approved for public release; distribution is unlimited.					
13. SUPPLEMENTARY NOTES The views, opinions and/or findings contained in this report are those of the author(s) and should not contrued as an official Department of the Army position, policy or decision, unless so designated by other documentation.					
14. ABSTRACT					
15. SUBJECT TERMS					
16. SECURITY CLASSIFICATION OF:			17. LIMITATION OF ABSTRACT UU	15. NUMBER OF PAGES	19a. NAME OF RESPONSIBLE PERSON Dmitri Donetski
a. REPORT UU	b. ABSTRACT UU	c. THIS PAGE UU			19b. TELEPHONE NUMBER 631-632-8411

RPPR Final Report
as of 07-Jan-2020

Agency Code:

Proposal Number: 68326EL

Agreement Number: W911NF-16-2-0053

INVESTIGATOR(S):

Name: Dmitri Donetski
Email: dmitri.donetski@stonybrook.edu
Phone Number: 6316328411
Principal: Y

Name: Gregory Belenky Ph.D.
Email: gregory.belenky@stonybrook.edu
Phone Number: 6316329741
Principal: N

Name: Sergey Suchalkin
Email: sergey.suchalkin@stonybrook.edu
Phone Number: 6316328413
Principal: N

Organization: **Research Foundation of SUNY at Stony Brook University**

Address: W-5510 Melville Library, Stony Brook, NY 117943362

Country: USA

DUNS Number: 804878247

EIN: 141368361

Report Date: 05-Jan-2020

Date Received: 05-Jan-2020

Final Report for Period Beginning 06-Apr-2016 and Ending 05-Oct-2019

Title: Novel metamorphic heterostructures for long wave infrared optoelectronics

Begin Performance Period: 06-Apr-2016

End Performance Period: 05-Oct-2019

Report Term: 0-Other

Submitted By: Dmitri Donetski

Email: dmitri.donetski@stonybrook.edu

Phone: (631) 632-8411

Distribution Statement: 1-Approved for public release; distribution is unlimited.

STEM Degrees: 1

STEM Participants: 5

Major Goals: III-V semiconductor compound barrier heterostructures for infrared optoelectronics are considered to be an attractive alternative to II-VI (HgCdTe) technology, mainly because of the lower cost, ease of scaling to large format arrays and better uniformity [1]. Due to the stronger, less ionic chemical bond, III-V semiconductors are more robust and stable than their II-VI equivalents. During SPIE Defense and Security Conference in April 2017, Anaheim, California, the spectacular results of the Vital Infrared Sensor Technology Acceleration (VISTA) US government program in developing Type-2 Strained Layer Superlattice (SLS) Focal Plane Array of small pixel detectors have been demonstrated. Optoelectronic devices with Type-2 InAsSb/InAs (Ga-free) SLS absorbers grown lattice matched to GaSb substrate outperform previously employed technologies in mid-wave infrared (MWIR) wavelength range. At the same time, extension of Type-2 Ga-free SLS operation to Long Wave Infrared Range (LWIR) meet fundamental challenges [2]. Reduction of the energy gap in this system and increase of cut-off wavelength, respectively, is obtained with increase of Sb composition. Following this approach for reliable device operation, the practical Sb composition in InAsSb is limited to ~40 % defined by the maximum 2 % strain in InAsSb layer grown lattice matched to GaSb. This leads to an increasing challenge to obtain the device cut-off wavelength beyond 12 μm . A consequence of large Sb composition in InAsSb layers is an increase of the thickness of InAs layers dictated by required strain balancing with growth on the GaSb platform. Elevated thickness of InAs layers results in reduction of electron hole overlap (lower absorption) and impeded hole transport (shorter minority hole diffusion length in the growth direction). Both of the factors result in reduction of the critical parameter, quantum efficiency.

In our solution solution we eliminate the design constraint implied by GaSb lattice constant by developing GaInSb and AlInSb virtual substrates (VS) with elevated lattice constants. The latter allows an increase of the average Sb composition in the device absorber and realization of energy gaps approaching zero for removing cut-off wavelength limit as well as realization of absorbers with inverted bands for novel properties useful for device applications. With the VS approach the InAsSb x/InAsSby SLS absorbers can be designed with short periods for a

RPPR Final Report as of 07-Jan-2020

superior e-h wavefunction overlapping resulting in a bulk-like absorption and unimpeded hole transport in the growth direction.

Major Goals:

1. To explore a new way to device engineering lifting the design limitations dictated by the substrate and making the lattice constant a design parameter.
To design III-V semiconductor compound heterostructures with energy gaps below 0.1 eV with combination of novel and unique optical and carrier transport properties including high optical absorption and long diffusion length of minority holes in the growth direction.
2. To assess the role of naturally-formed CuPt-type ordering in engineering InAsSbx/InAsSby epitaxial heterostructures.
3. To determine energy gap and energy dispersion parameters of heterostructures with energy gaps below 0.1 eV with magneto-absorption and magneto-transport measurements in strong magnetic fields.

Developing of the optimal VS buffer technology for high quality epitaxy on lattice mismatched substrates, understanding the role of ordering in epitaxial growth of InAsSb -based absorbers are important fundamental studies toward integration of the MWIR and LWIR optoelectronic materials on GaAs and Si platforms.

References:

1. A. Rogalski, P. Martyniuk, M. Kopytko, Type-II superlattice photodetectors versus HgCdTe photodiodes, Conference: Sensors, Systems, and Next-Generation Satellites XXIII, October 2019, DOI: 10.1117/12.2538538
2. D. Ting, A. Soibel, A. Khoshakhlagh et al, Development of InAs/InAsSb Type II Strained-Layer Superlattice Unipolar Barrier Infrared Detectors, J. of Electron. Mater., 48 (10), 2019. DOI: 10.1007/s11664-019-07255-x

Accomplishments: Quality InAsSb-based epitaxial layers and barrier heterostructures of nBn and nBp types with average Sb compositions significantly greater than 10 % have been grown by Molecular Beam Epitaxy on GaSb and GaAs platforms. A near 10 % average Sb composition is realized with conventional pseudomorphic growth with lattice matching of InAsSb SLS to the GaSb substrate. A larger average Sb composition requires a buffer with a larger lattice constant compared to that of GaSb. The lattice constant difference was accommodated with GaInSb and AlInSb buffers and VS with the lattice constant up to 6.33 Å. This implies the metamorphic growth of the buffer with a near complete relaxation of the buffer layer and unrelaxed unstrained VS on the top of the buffer to enable quality growth of the InAsSb-based absorber. The energy gaps of barrier heterostructure absorbers with GaInSb buffers corresponded to wavelength range from 9 to 14 μm at T = 77 K. The absorbers with energy gaps approaching zero and with inverted bands were grown with AlInSb buffers. The absorber thickness was in the range from 1 to 3 μm. An InAsSbx/InAsSby SLS system can be considered as an alloy with engineered group V composition ordering along the growth axis. The absorber materials have been structurally characterized by high resolution X-ray diffractometry with Reciprocal Space Mapping (RSM), Transmission Electron Microscopy (TEM). The impact of strain on the natural ordering was studied by electron diffraction. The energy gaps of the absorbers at T = 4 K were determined by magnetoabsorption. Temperature dependencies of energy gaps in the temperature range up to 200 K were determined by fitting the photoluminescence spectra. The fundamental absorption spectra were determined from optical transmission. The minority hole lifetime and vertical transition time in the absorbers of barrier heterostructures were determined from the transient response to a pulsed laser excitation in the temperature range from 77 to 200 K.

A significant effort was made in optimization of the barrier layer design and growth regime for minimization of the valence band offset between the barrier and absorber layers in nBn heterostructure. The barrier composition was varied in a set of nBn heterostructures and the dependences of response versus bias were measured. Both bulk and short-period SLS barrier designs were employed. The minimal bias of 0.25 V was obtained for nBn heterostructures grown without interruption at the interface of the barrier and absorber. This bias value was consistent with our expectations considering a 1×10^{17} 1/cm³ doping level of the top contact and background absorber concentration of $(1-3) \times 10^{15}$ 1/cm³ level which results in the barrier for hole at equilibrium conditions.

The InAsSb-based heterostructures with high average Sb compositions were shown to have the LWIR absorption up to a factor of 3 greater compared to that in InAsSb/InAs SLS with average Sb composition about 10 % required with the lattice matched growth on GaSb. The superior absorption translates to improvement of the LWIR device quantum efficiency (QE) and can be traded for reduction of the absorption thickness. At the same time, the heterostructures with high average Sb compositions show the corresponding reduction of transport time across the absorber due to improved hole transport.

The hole diffusion lengths in a range of 10 μm were determined by separation of fast and slow parts of transient

RPPR Final Report

as of 07-Jan-2020

responses of barrier heterostructures. The minority hole lifetime of 0.55 μ s at $T = 77$ K was obtained for 2 μ m undoped SLS absorbers with the average Sb composition of 36 % and the energy gap corresponding to the wavelength of 9 μ m.

With a microsecond scale minority hole lifetime and a bulk-like fundamental absorption the developed absorbers properties approach those for the state-of-art HgCdTe with the addition of advantages of heterobarrier technology for blocking majority electron current and reduction of the impact of the depletion region in the absorber on the dark current. A long hole diffusion length makes a room for trading it up for scaling down the dark current and/or increase of the device operating temperature. To assess the fundamental Auger recombination properties of the absorbers, the modulation of the LWIR transmission of the nBp heterostructures with a 85 meV energy gap was studied in the temperature range from 77 to 200 K under pulsed current injection of excess carriers. The excess carrier concentrations were determined by modeling. It was found that the Auger coefficient values were following that for CHCC process in HgCdTe alloys of similar energy gaps with excess carrier concentrations up to the level of $1E16$ 1/cm³ in the entire temperature range.

The lateral photoconductivity (PC) of InAsSbx/InAsSby SLS was studied in the heterostructures where the SLS layer was enclosed with lightly p-doped AlInSb carrier confinement layers. A significant reduction of the PC was observed compared to that in heterostructures with vertical carrier transport. Under higher excitation a negative PC was observed. The phenomenon was explained with a rapid reduction of the electron mobility with increase of the quasi-Fermi level due to both optical phonon scattering and strong non-parabolicity of the conduction band in the narrow gap SLS. The phenomenon showed the practical importance of the barrier heterostructure design with blocking the majority carrier transport.

The electron effective masses and the mass dispersion were determined by magneto optical measurements. We demonstrated that in metamorphic superlattices the ultra-narrow bandgaps (< 100 meV) can be reached at SLS periods which are much shorter than in a typical pseudomorphic InAsSb SLS. A zero energy bandgap can be realized in the SLs with a typical period around 6 nm.

We found that nearly gapless short-period metamorphic InAsSb SLS manifest a new class of Dirac materials with controllable Fermi velocity. We applied direct experimental method to probe the carrier dispersion and the bandgap, such as magneto-absorption, magneto-transport and angle-resolved photoemission spectroscopy (ARPES). The latter had never been used before on SLS materials. The energy dispersion was determined from the peaks of cyclotron resonance. The cyclotron energy was found to be proportional to a square root of the magnetic field which is a direct indication to the linearity of the carrier energy dispersion. The Dirac-type dispersion was confirmed by the ARPES data. The TEM imaging and transport measurements demonstrate high quality, dislocation-free material which can be used for quantum device applications. Further increase of the ordering period leads to band inversion and opening hybridization gap at the Γ point. We developed a model for calculation of in-plane and vertical carrier energy dispersion in metamorphic short-period InAsSb-based superlattices based on NextNano software. The material parameters were obtained from magneto-absorption measurements performed on the bulk InAsSb alloys with various compositions. The model takes into account interface disorder, which is seen on high resolution TEM images. With this system intriguing physics phenomena, such as nontrivial topological phases can be realized.

The obtained data proved that metamorphic InAsSbx/InAsSby short-period SLS can be a new platform for long-wave infrared optoelectronics.

RPPR Final Report as of 07-Jan-2020

Training Opportunities: Training opportunities

The results were presented at the following conferences and meetings

1. D. Donetski, J. Liu, G. Kipshidze, G. Belenky, W. L. Sarney, S. P. Svensson, "Measurements of carrier transport time in InAsSb-based SLS", Center for Semiconductor Modeling Consortium, Annual meeting, Boston University, October 15, 2019.
2. W.L. Sarney, S.P. Svensson, A.C. Leff, D. Donetsky, "Influence of strain on InAsSb composition", The 35th North American Conference on Molecular Beam Epitaxy (NAMBE 2019), Ketchum, ID, September 22-25, 2019.
3. W.L. Sarney, S.P. Svensson, A.C. Leff, D. Donetsky, G. Kipshidze, L. Shterengas, G. Belenky, "Grading for ultimate design control of semiconductor device structures", The 35th North American Conference on Molecular Beam Epitaxy (NAMBE 2019), Ketchum, ID, September 22-25, 2019.
4. S. Suchalkin, G. Belenky, L. Shterengas, B. Laykhtman, G. Kipshidze, M. Ermolaev, D. Smirnov, J. Ludwig, S. Moon, D. Graf, S. Svensson, W. Sarney "Metamorphic InAs_{1-x}Sb_x/InAs_{1-y}Sb_y superlattices with ultra-low bandgap as a Dirac material" Invited seminar talk in Hard Condensed Matter Seminar, Georgia Institute of Technology, August 24, 2017.
5. S. Suchalkin, G. Belenky, L. Shterengas, B. Laykhtman, G. Kipshidze, M. Ermolaev, D. Smirnov, J. Ludwig, S. Moon, D. Graf, S. Svensson, W. Sarney (invited), "Properties of novel metamorphic III-V materials with ultralow bandgaps", SPIE Photonics West, S. Francisco, CA, USA, 2017.
6. S. Suchalkin, G. Belenky "Metamorphic ordered InAsSb alloys: a new platform for topological electronics and IR optoelectronics" (invited), Modern Trends in Condensed Matter Physics, September 24-26, 2018 Baku, Azerbaijan
7. S. Suchalkin, G. Belenky, M. Ermolaev, S. Moon, Y.X. Jiang, D. Graf, D. Smirnov, B. Laikhtman, L. Shterengas, G. Kipshidze, S.P. Svensson, W.L. Sarney, "Metamorphic strain-compensated InSb/InAsSb superlattices with ultra-thin layers" (invited), NAMBE-2018, September 30 – October 5, 2018, Banff, Canada.
8. S. Suchalkin, M. Ermolaev, T. Valla, G. Kipshidze, D. Smirnov, S. Moon, Z. Jiang, Y. Jiang, S. P. Svensson, W. L. Sarney and G. Belenky "Quantum materials based on metamorphic InAsSb superlattices" (invited) IEEE RAPID, September 2019, Miramar Beach, FL, USA
9. Y. Xu, A. Frenkel, Y. Lin, D. Donetsky, S. Suchalkin, L. Shterengas, G. Kipshidze, G. Belenky, S. P. Svensson and W. L. Sarney, "Carrier lifetime and photoconductivity measurements in short-period InAsSb-based SLS grown on metamorphic buffers", Electronic Materials Conference EMC-59, University of Notre Dame, South Bend, IN, Student talk, Presenter: Catherine Ye Xu, June 2017.

In the reporting period 3 Ph.D., 1 M.S. and 1 undergraduate students were involved in the experimental and modeling efforts of the projects. One Ph.D. student has completed the Ph.D. program and defended the dissertation. Two PhD students are preparing their dissertations for defense. 3 graduate students participated in modeling of the energy spectra of the InAsSb_x/InAsSb_y SLS, high resolution XRD characterization of the grown structures, determination of the materials compositions and strain, processing heterostructures for optical and carrier transport measurements, computerized data collection, data analysis, preparation of technical reports and presentation of results at the conferences. Two graduate students co-authored the conference talks (SPIE Photonics West and EMC) and attended the above conferences, one student made a presentation at the EMC. Two undergraduate students participated in modeling of the energy spectra of SLS, modeling of the negative photoconductivity effect in SLS and the mask design for processing of heterostructures.

RPPR Final Report as of 07-Jan-2020

Results Dissemination: 1. A press release by Army Research Laboratory, January 11, 2018, "Army scientists shed light on new low-cost material for seeing in the dark" highlighted the collaborative work of ARL and Stony Brook University groups.

This publication was referenced in several articles published online: Phys.org, January 11, 2018, under the title above.

Semiconductor today, January 12, 2018, "US Army and Stony Brook grow InAsSb on GaAs substrates using GaSb intermediate defect-trapping layer and graded buffer"

CS Compound Semiconductors, January 17, 2018, "Army Scientists Use InAsSb To Make IR Sensors".

ArmyTimes, January 21, 2018, "Army scientists devise new way to make night vision cheaper, better"

Laser Focus World, February 16, 2018, "U.S. Army Research Laboratory and Stony Brook develop lower-cost night-vision material".

Compound Semi, February 19, 2018, "ARL scientists realized material had to be undistorted by strain".

2. A seminar has been held at the Dept. of ECE, Stony Brook University February 27, 2018, with 4 presentations:

- Stefan Svensson, Wendy Sarney (ARL) "In-situ Al metallization of narrow bandgap III-V materials for studies of proximity superconductivity"
- Dmitri Donetski (SBU) "Carrier recombination and transport in barrier heterostructures"
- Sergey Suchalkin (SBU) "Carrier dispersion and transport in InAsSb alloys with periodic composition modulation"
- Leon Shterengas (SBU) "Laser photonic crystal design and technology"

3. Joint seminar of Army Research Laboratory and Stony Brook University: Presenters: Dr. Wendy Sarney, Dr. Stefan Svensson, Prof. Dmitri Donetski, Prof. Sergey Suchalkin, Stony Brook University, July 2017.

4. Joint seminar of Jet Propulsion Laboratory and Stony Brook University, Presenters: Dr. Alex Soibel, Prof. Sergey Suchalkin, May 2017.

5. Seminar at Stony Brook with Prof. Sanjay Krishna, Ohio State University, November 2016.

6. Seminar at the Georgia Tech University, August 2017. Presenter: Prof. Sergey Suchalkin, Invited talk.

Honors and Awards: Nothing to Report

Protocol Activity Status:

Technology Transfer: The research effort was conducted in close collaboration with the US Army Research Laboratory scientists Dr. Stefan P. Svensson and Dr. Wendy L. Sarney.

PARTICIPANTS:

Participant Type: PD/PI

Participant: Dmitri Donetski

Person Months Worked: 1.00

Project Contribution:

International Collaboration:

International Travel:

National Academy Member: N

Other Collaborators:

Funding Support:

RPPR Final Report
as of 07-Jan-2020

Participant Type: Co PD/PI
Participant: Gregory Belenky
Person Months Worked: 1.00
Project Contribution:
International Collaboration:
International Travel:
National Academy Member: N
Other Collaborators:

Funding Support:

Participant Type: Co PD/PI
Participant: Sergey Suchalkin
Person Months Worked: 1.00
Project Contribution:
International Collaboration:
International Travel:
National Academy Member: N
Other Collaborators:

Funding Support:

Participant Type: Co-Investigator
Participant: Gela Kipshidze
Person Months Worked: 3.00
Project Contribution:
International Collaboration:
International Travel:
National Academy Member: N
Other Collaborators:

Funding Support:

Participant Type: Faculty
Participant: Leon Shterengas
Person Months Worked: 1.00
Project Contribution:
International Collaboration:
International Travel:
National Academy Member: N
Other Collaborators:

Funding Support:

Participant Type: Graduate Student (research assistant)
Participant: Ye Xu
Person Months Worked: 12.00
Project Contribution:
International Collaboration:
International Travel:
National Academy Member: N
Other Collaborators:

Funding Support:

Participant Type: Graduate Student (research assistant)
Participant: Jinghe Liu
Person Months Worked: 6.00
Project Contribution:
International Collaboration:
International Travel:
National Academy Member: N
Other Collaborators:

Funding Support:

RPPR Final Report
as of 07-Jan-2020

Participant Type: Graduate Student (research assistant)

Participant: Zichen Zhang

Person Months Worked: 2.00

Funding Support:

Project Contribution:

International Collaboration:

International Travel:

National Academy Member: N

Other Collaborators:

Participant Type: Consultant

Participant: Boris Laikhtman

Person Months Worked: 1.00

Funding Support:

Project Contribution:

International Collaboration:

International Travel:

National Academy Member: N

Other Collaborators:

Participant Type: Undergraduate Student

Participant: Haiying Jiang

Person Months Worked: 1.00

Funding Support:

Project Contribution:

International Collaboration:

International Travel:

National Academy Member: N

Other Collaborators:

Participant Type: Graduate Student (research assistant)

Participant: Maksim Ermolaev

Person Months Worked: 12.00

Funding Support:

Project Contribution:

International Collaboration:

International Travel:

National Academy Member: N

Other Collaborators:

CONFERENCE PAPERS:

Publication Type: Conference Paper or Presentation

Publication Status: 1-Published

Conference Name: SPIE OPTO

Date Received: 31-Aug-2017

Conference Date: 28-Jan-2017

Date Published: 15-Jun-2017

Conference Location: San Francisco, California, United States

Paper Title: Properties of novel metamorphic III-V materials with ultra-low bandgaps (Conference Presentation)

Authors: Sergey Suchalkin, Gregory Belenky, Leon Shterengas, Boris Laykhtman, Gela Kipshidze, Maxim Ermolaev

Acknowledged Federal Support: **Y**

RPPR Final Report
as of 07-Jan-2020

Publication Type: Conference Paper or Presentation

Publication Status: 1-Published

Conference Name: Electronic Materials Conference

Date Received: 31-Aug-2017 Conference Date: 28-Jun-2017

Date Published: 28-Jun-2017

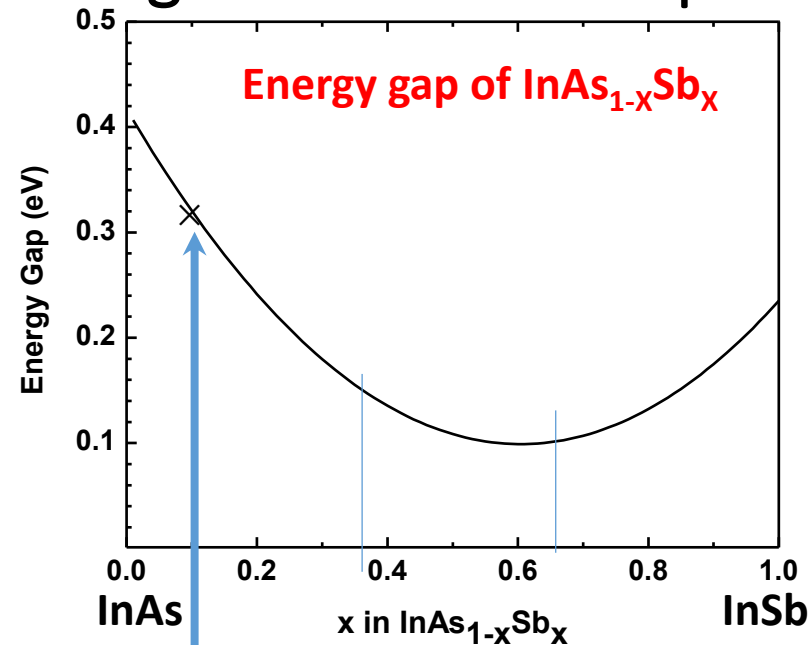
Conference Location: University of Notre Dame, South Bend, IN

Paper Title: Carrier lifetime and photoconductivity measurements in short-period InAsSb-based SLS grown on metamorphic buffers

Authors: Ye (Catherine) Xu, Alex Frenkel, Youxi Lin, Dmitry Donetsky, Sergey Suchalkin, Leon Shterengas, Gel:

Acknowledged Federal Support: **Y**

Novel Metamorphic Heterostructures for Long Wave Infrared Optoelectronics



Lattice constant (Å):

~6.1

6.2

6.33

Average Sb composition (%): ~10

36 ↔ 63

100

Conventional pseudomorphic growth lattice-matched to GaSb substrate

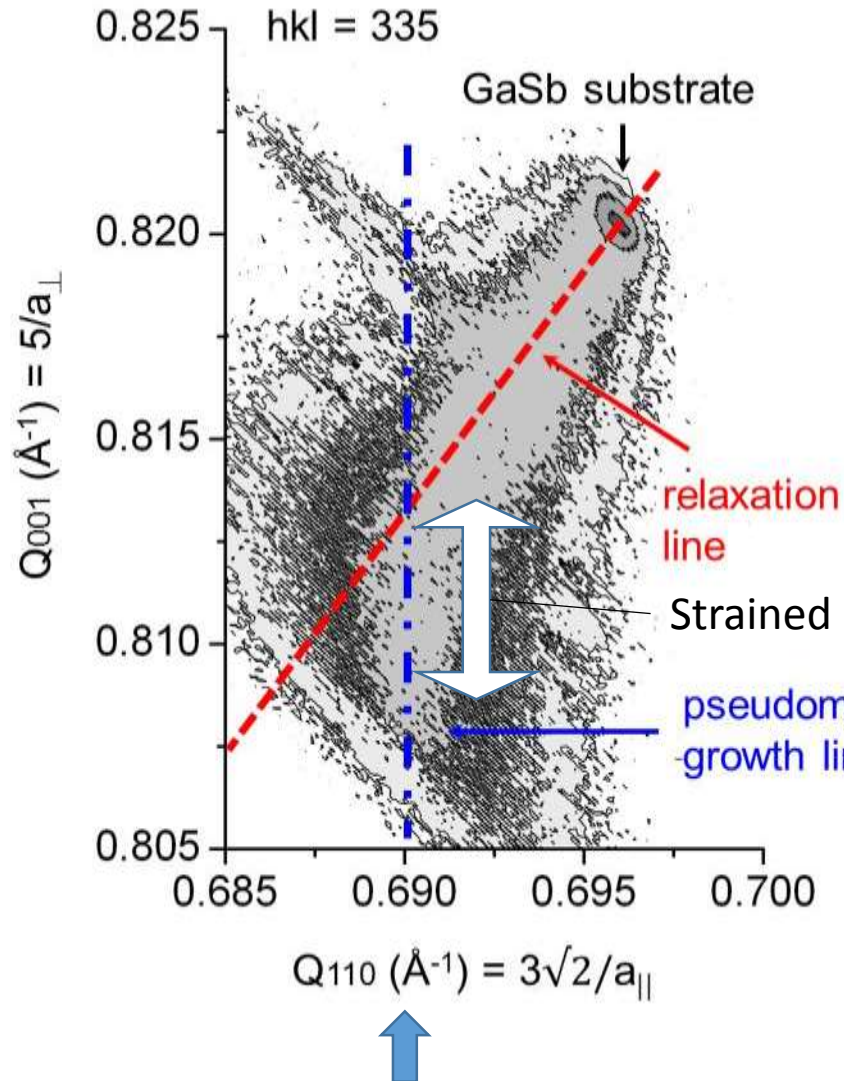
- Bulk InAsSb (Sb ~10%), $E_g \sim 0.33$ eV
 - InAs/InAsSb SLS (Sb ≤ 40%), $E_g \geq 0.1$ eV
- For reliability max Sb composition in SLS is limited by max strain of 2 %

Metamorphic growth pursued in this project:
Quality epilayers are grown lattice matched to GaInSb and AlInSb virtual substrates grown with metamorphic buffers on GaSb

- Bulk InAsSb (Sb = 40-60%), $E_g = 0.13 - 0.09$ eV
- InAsSbx/InAsSby SLS (average Sb=36-63%), $E_g \leq 0.1$ eV with typical strain ≤ 1 %

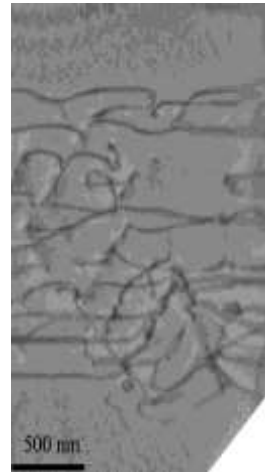
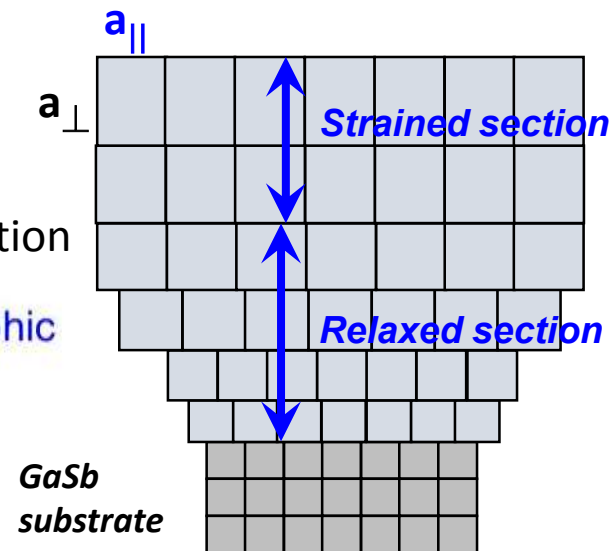


X-ray reciprocal space mapping



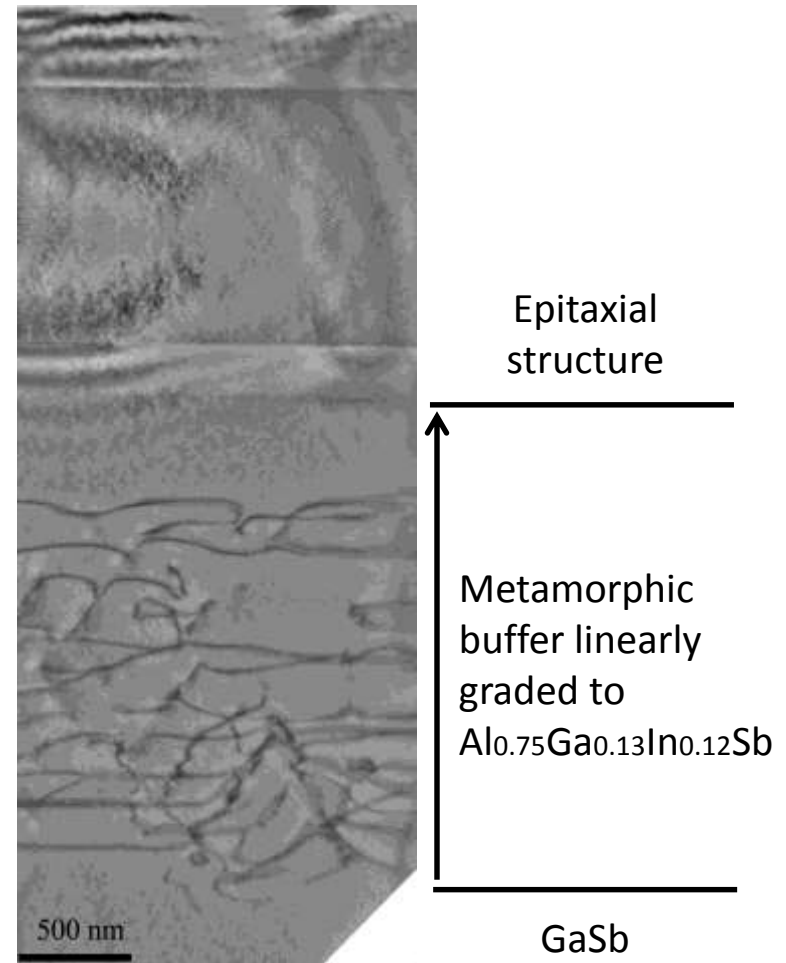
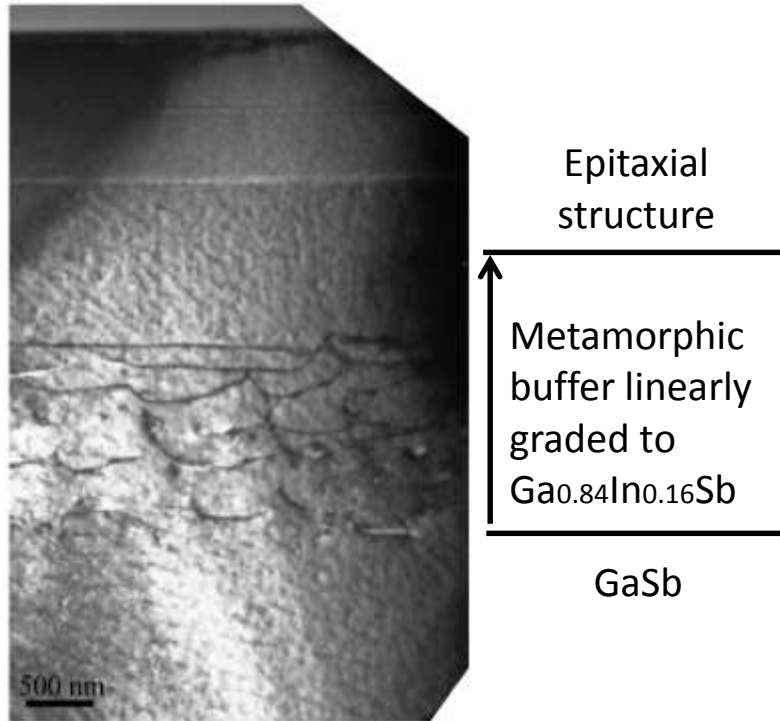
It is critical to determine the in-plane lattice parameter a_{\parallel} on top of the buffer.

The epilayer is grown with the lattice constant matching to a_{\parallel}



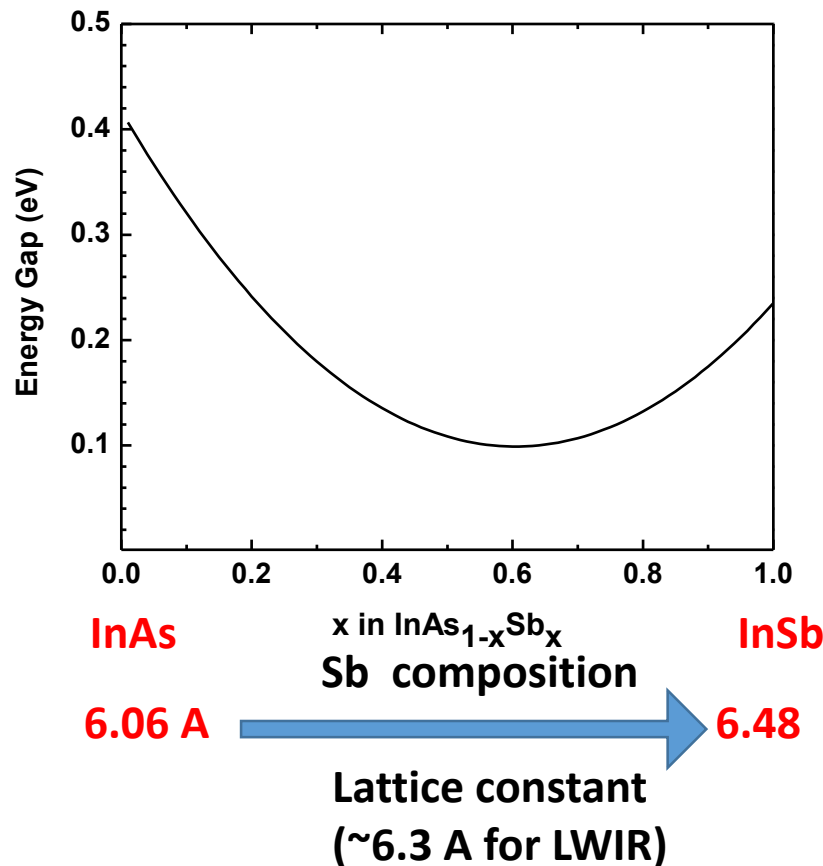
The line with lattice constant a_{\parallel} corresponds to the top active region (bulk, SLS)

$[001]$ \nearrow $[111]$ - preferred direction for threading dislocations
 \rightarrow $[110]$ - preferred direction for misfit dislocations



1. Dislocation networks confined in the bottom part of the buffer
2. Long horizontal lines indicate effective lateral glide of dislocations

A 90 meV energy gap of bulk $\text{InAs}_{0.4}\text{Sb}_{0.6}$ alloy at $T = 77\text{ K}$ qualifies the materials for high performance LWIR detector applications



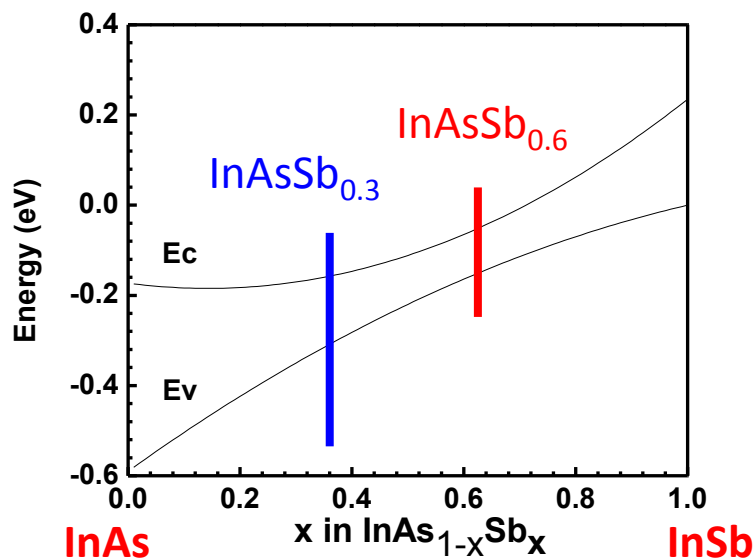
Advantages of bulk InAsSb alloys:

- Strong absorption similar to that of bulk HgCdTe alloys
- Abrupt absorption edge for Sb =50-60 % (no tail) due to independence of E_g from Sb fluctuations
- High minority hole mobility - twice greater than that in HgCdTe alloys
- Long minority carrier lifetime attributed to absence of Ga
- Energy band position ideally matching to AlSb-based alloys for design of barrier heterostructures

InAsSb-based compounds have a strong potential to surpass HgCdTe alloys in conventional and novel applications in LWIR wavelength range

Epitaxial growth of InAsSb with a lattice constant $\sim 6.3\text{ Å}$ on available 6.1 Å GaSb substrates required optimization of the design of metamorphic buffers between InAsSb and the substrate which allowed to obtain device quality epitaxial materials

Short-period InAsSb_x/InAsSb_y SLS -III-V compounds for superior VLWIR detectors

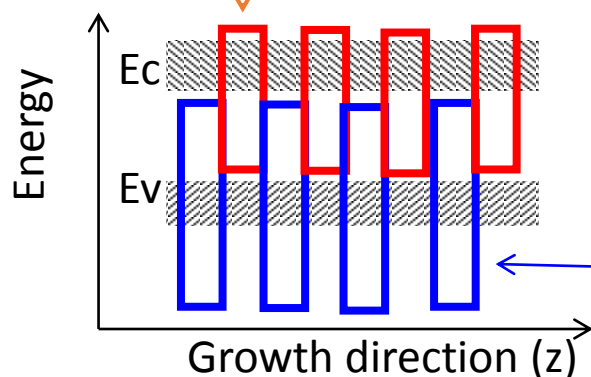


Short-period strained layer superlattices (SLS) with various properties were developed by modulation of Sb composition during growth

- energy bandgaps below 0.1 eV
- strong fundamental absorption as in bulk alloys
- unimpeded hole transport
- linear energy dispersion $E(k)$
- inverted bands ($E_v > E_c$) with flattened dispersion near the bottom (high effective mass)

Implemented design: InAsSb_{0.3}/InAsSb_{0.6} SLS with short periods (2.3 – 5.4 nm)

InAsSb_{0.6} (1 % compressive strain)



- Bulk-like absorption spectrum due to 95 % overlap of the electron-hole wave functions
- Small energy gaps: response to $\lambda \sim 20 \mu\text{m}$ and beyond
- Wide hole minibands ensure efficient hole transport

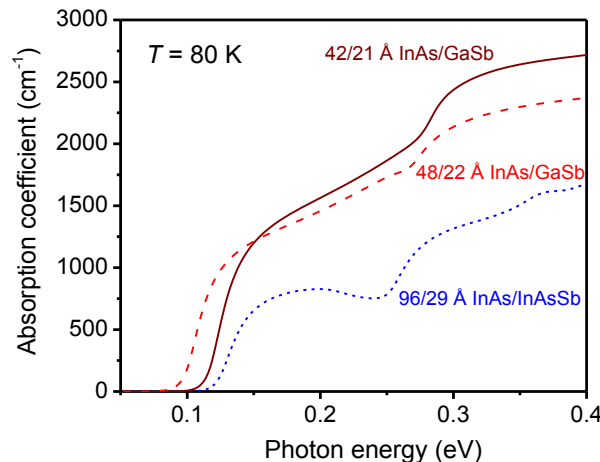
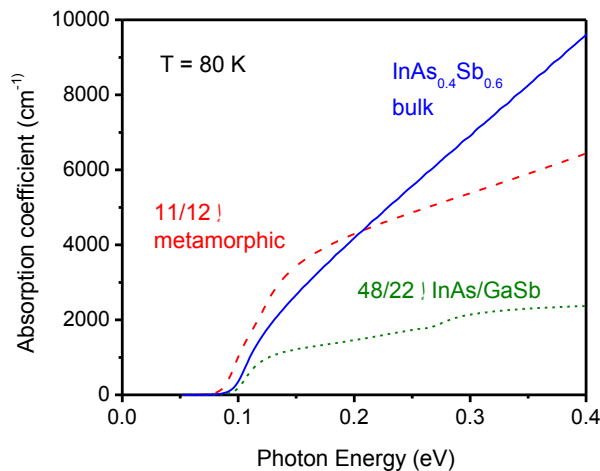
Hole miniband width:

120 meV for SLS with 2.3 nm period

40 meV for SLS with 3.2 nm period

Short-period SLS and bulk InAsSb show the highest absorption.

In pseudomorphic SLS the absorption is a factor of 2 to 3 lower.



In LWIR range the fundamental absorption of short period InAsSb-based SLS grown metamorphically is similar to that of bulk alloys: InAsSb and HgCdTe. At $\lambda = 8 \mu\text{m}$ (photon energy = 0.15 eV) the bulk and short –period SLS absorption is $(2.5\text{-}3) \times 10^3 \text{ cm}^{-1}$.

The fundamental absorption in **InAs/GaSb** SLS grown pseudomorphically on GaSb is $\sim 1.2 \times 10^3 \text{ cm}^{-1}$. It is a factor of two smaller than that for short period InAsSb-based SLS.

For **Ga-free InAs/InAsSb** SLS grown pseudomorphically on GaSb the fundamental absorption is $\sim 700 \text{ cm}^{-1}$. It is a factor of 3 smaller than that for short period SLS grown on metamorphic buffers.

Under all conditions being equal one can expect greater quantum efficiencies for devices grown with the metamorphic buffer approach.

Pseudomorphic vs Metamorphic growth

At the initial growth stage heteroepitaxial growth is pseudomorphic . The elastic energy of deformation due to misfit of lattice constants is stored in the epilayer lattice. In thin layers strain up to 2 % can be realized. On GaSb substrate one can grow pseudomorphically GaInAs with up to 20 % of Ga or InAsSb with up to 55 % of Sb. Total strain in compressive and tensile strained layers has to be carefully balanced.

For LWIR application the energy gap constraint significantly limits the choice of layer compositions and thicknesses which saturates further improvement of the device design.

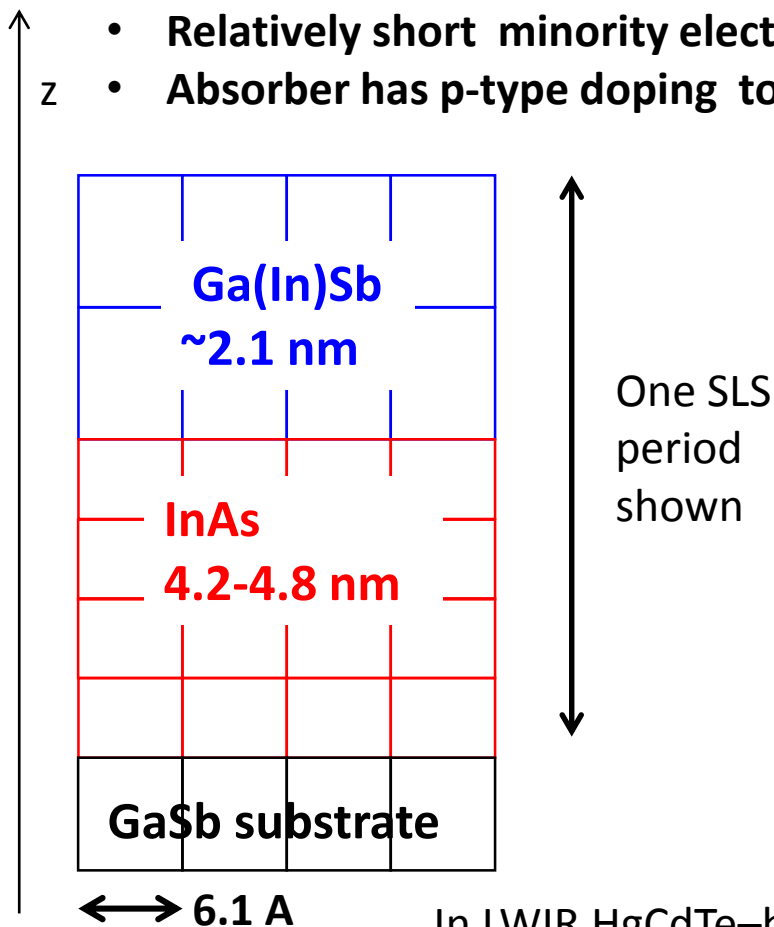
Significant improvement can be obtained with metamorphic growth with change of the lattice constant. Mismatched buffer heterostructures are used to improve device performance of high electron mobility transistors, heterojunction bipolar transistors, multi-junction solar-cells.

The following two viewgraphs present major limitations in design of LWIR detectors for pseudomorphic growth on GaSb. These limitation are lifted with metamorphic growth when the lattice constant becomes a free design parameter.

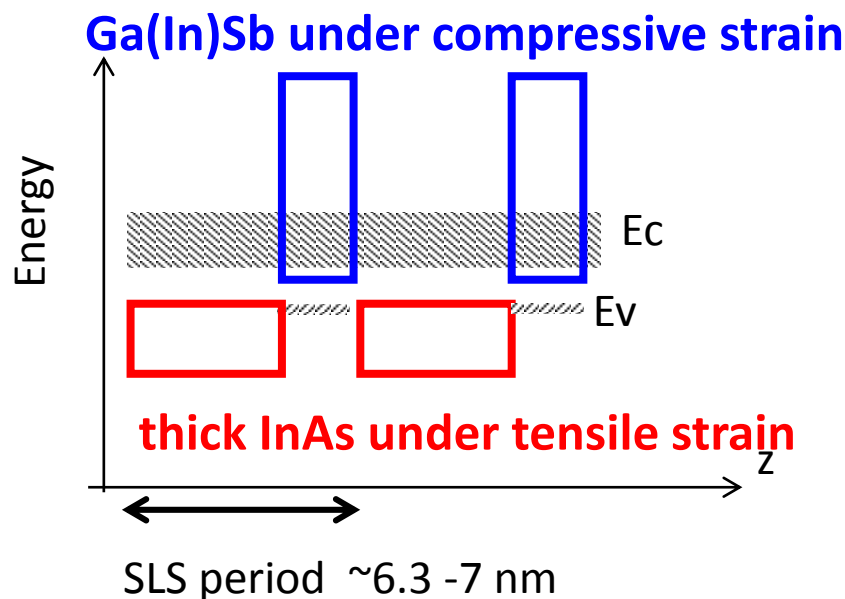
LWIR InAs/Ga(In)Sb SLS grown pseudomorphically on GaSb exhibit ~ 2 times lower absorption compared to bulk alloys



- For LWIR InAs layers have to be thick which results in hole confinement in Ga(In)Sb, reduced overlap of electron and hole wavefunctions and lower absorption
- Relatively short minority electron lifetime is attributed to presence of Ga.
- Absorber has p-type doping to take advantage of fast unimpeded electron transport.



Rectangles in energy band diagrams below denote the energy gaps of SLS cell materials

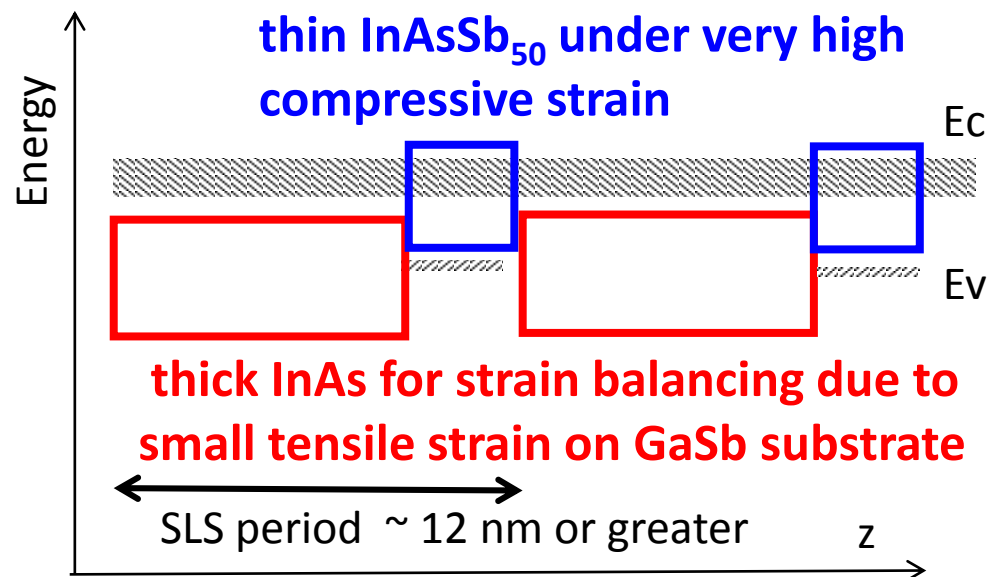
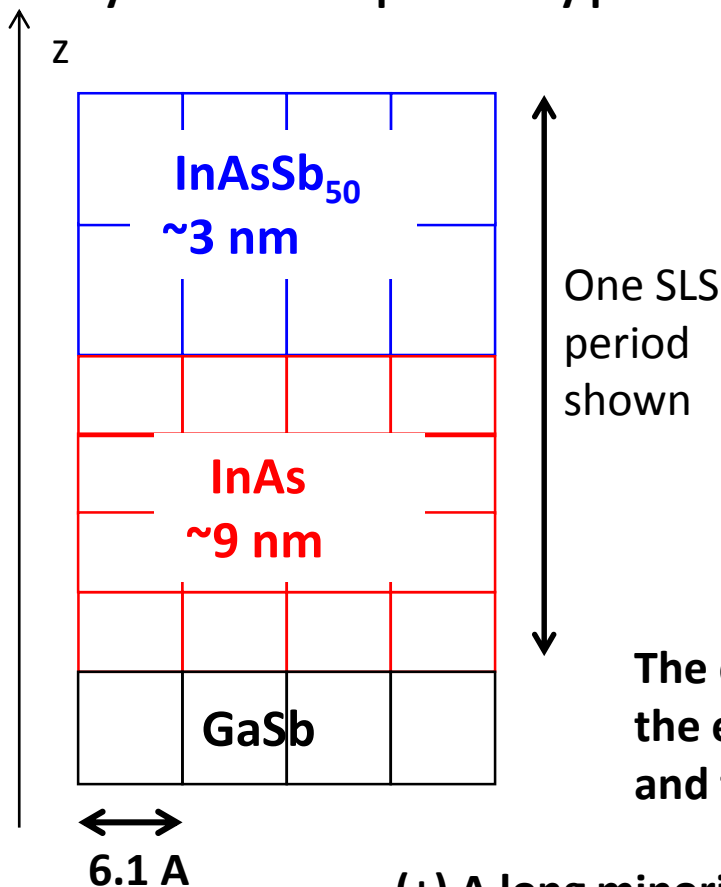


In LWIR HgCdTe-based devices offer better performance compared to Ga(In)Sb/InAs SLS. The substrate lattice constant constraint prevents significant improvement of the SLS design.

LWIR InAs/InAsSb SLS grown pseudomorphically on GaSb show ~3 times lower absorption compared to bulk alloys



Extension of the response to longer than 10 μm cut-off wavelength is limited by amount of practically possible compressive strain in Sb-rich InAsSb grown on GaSb.



The contribution of hole quantization energy in InAsSb to the energy gap limits the minimal width of InAsSb layer and that of InAs, respectively, for strain balance.

(+) A long minority carrier lifetime is attributed to Ga-free absorber

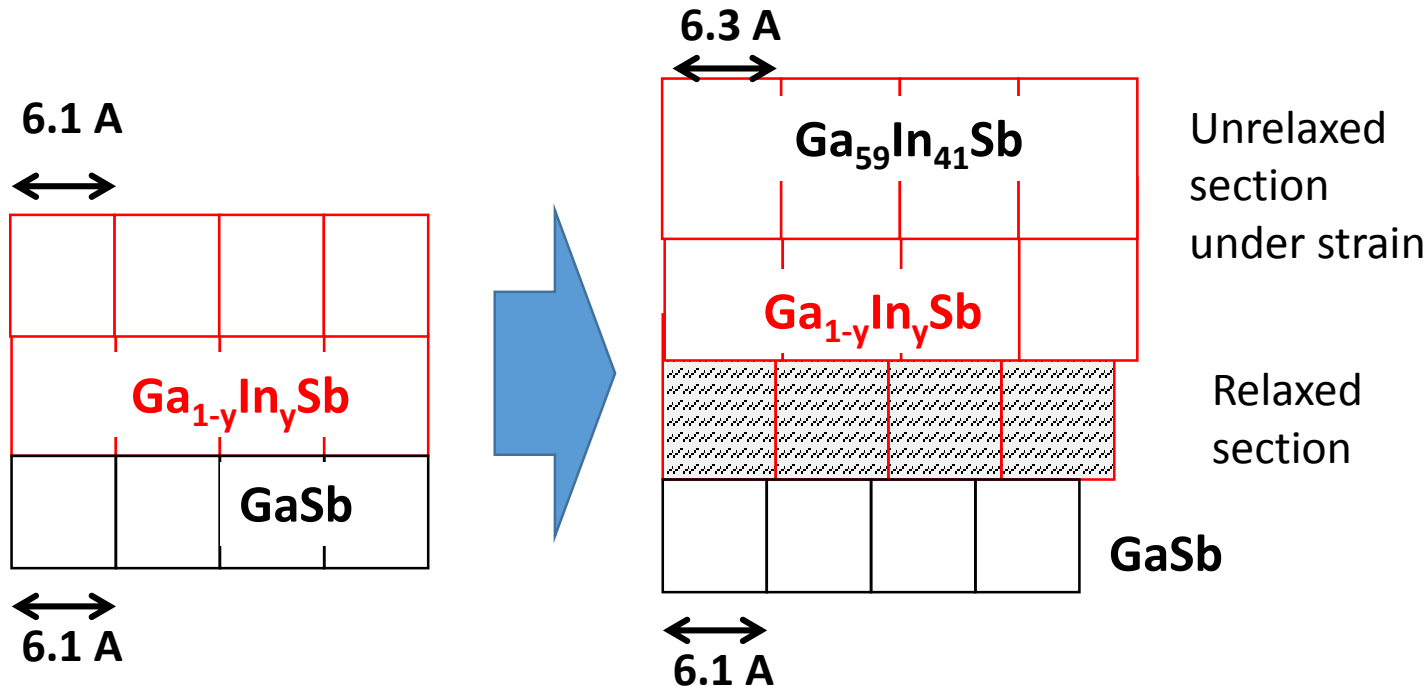
Holes are strongly confined in the InAsSb layers :

(-) Small electron-hole wavefunction overlap leads to lower absorption

(-) Impeded minority hole transport is due to thick InAs layers

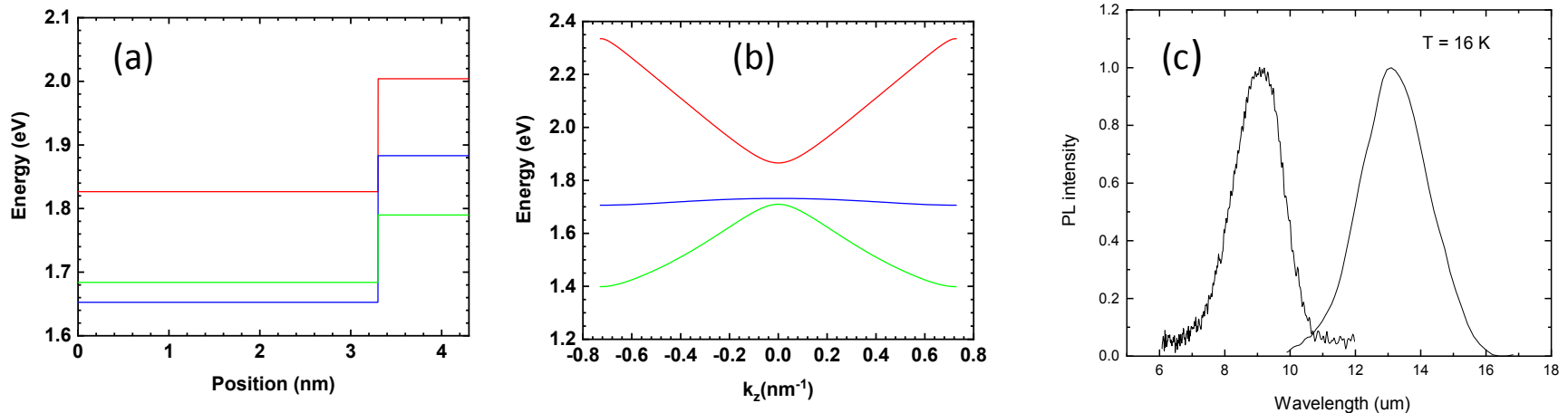
Metamorphic growth of linearly graded $\text{Ga}_{1-y}\text{In}_y\text{Sb}$ buffers

At the initial growth stage heteroepitaxial growth is pseudomorphic and the elastic energy of deformation is stored in the epilayer lattice (the left figure).



Upon reaching the critical thickness dislocations are formed with strain relaxation at the bottom at the interface of the epilayer and the substrate. The top layer of the buffer increments the lattice constant and reduces the strain (the center figure). The metamorphic growth is continued preserving the top layer unrelaxed. Dislocations are promoted to glide away in the lateral direction (TEM on the right). Quality unstrained InAsSb layer is grown lattice-matched to the top of the buffer.

Modeling of the energy band diagram and dispersion Agreement with low temperature PL spectra

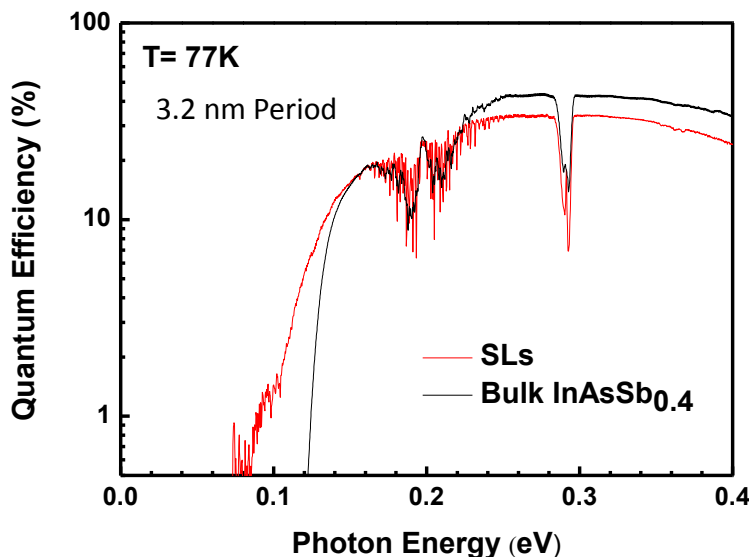
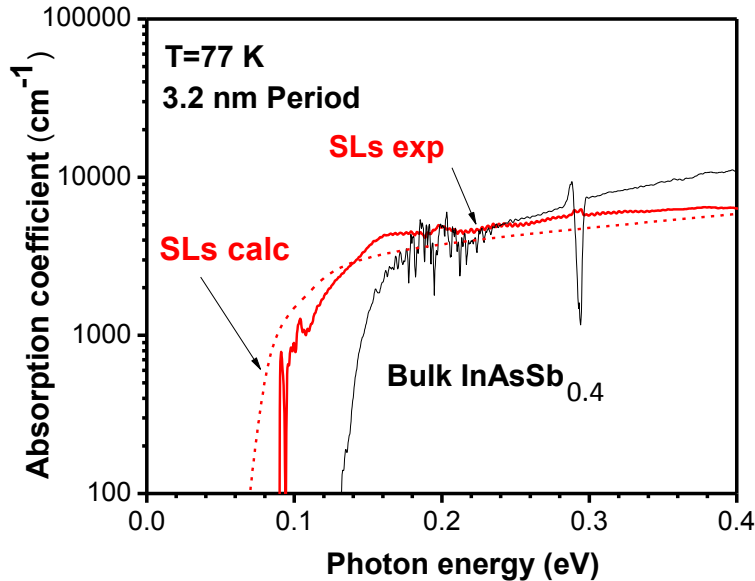


Modeling of the energy band and dispersion have been developed based on NextNano software. The material parameters have been adjusted based on experimental photoluminescence spectra. Matching of the calculated and measured energy gaps have been obtained in LWIR range of energies.

- (a) Conduction and valence band Energy levels for a 3.3 nm $\text{InAs}_{0.7}\text{Sb}_{0.3}$ / 1 nm $\text{InAs}_{0.45}\text{Sb}_{0.55}$ SLS
- (b) Energy dispersion for the above SLS design
- (c) Low temperature PL spectra for short period SLS grown on metamorphic buffers. The PL peak on left is for the above design. The PL peak on right is for the following design: 1.6 nm $\text{InAsSb}_{0.3}$ / 1.6 nm $\text{InAsSb}_{0.6}$ SLS



Experimental absorption and quantum efficiency spectra for LWIR bulk and SLS barrier heterostructures with 1- μm thick absorbers



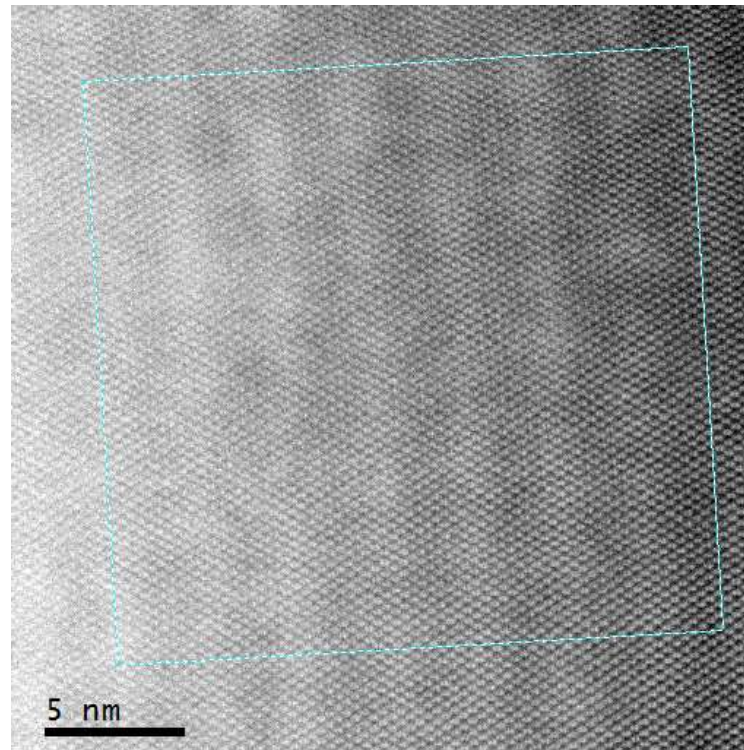
The experimental absorption in short-period SLS grown with metamorphic buffers matches to calculated values and values in bulk alloys.

The quantum efficiency obtained with short-period SLS absorbers was similar to those obtained with bulk absorbers. It means that hole mobility in short-period SLS was high enough to collect most generated carriers.

Significant reduction of dark current in heterostructures with bulk InAsSb absorbers was obtained with the absorber doping to 10^{16} cm^{-3} .

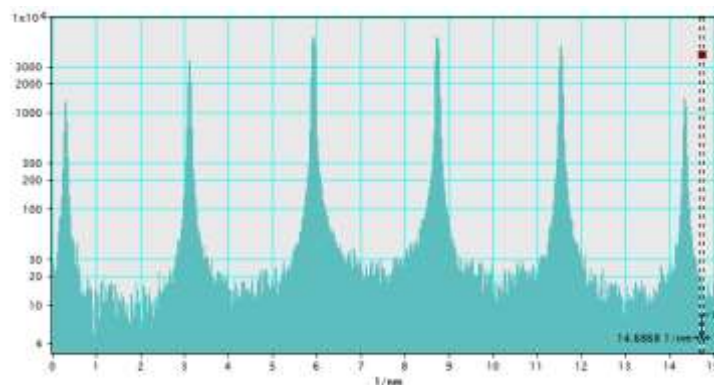
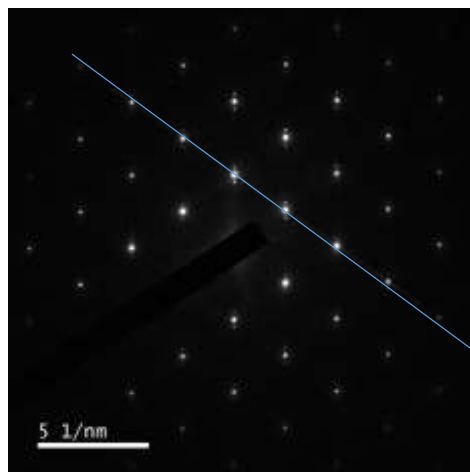
For these heterostructures with 1- μm thick InAsSb₄₀ absorbers the dark current density of $2 \times 10^{-5} \text{ A/cm}^2$ at T=77 K and a 50 MHz (-3 dB) response bandwidth consistent with high hole mobility were demonstrated. In the temperature range above 100 K the dark current was found to be diffusion limited.

Transmission Electron Microscopy Image of a 3.16 Å $\text{InAsSb}_{0.25}/\text{InAsSb}_{0.55}$ SLS grown on GaInSb metamorphic buffer

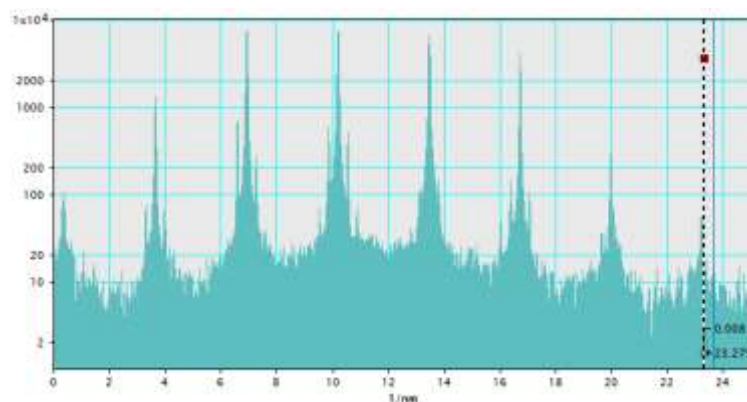
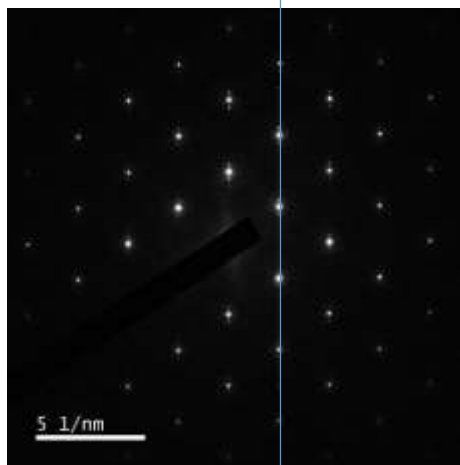


Measured in ARL

Electron diffraction in the 3.16Å $\text{InAsSb}_{0.25}/\text{InAsSb}_{0.55}$ SLS grown on GaInSb metamorphic buffer



No evidence of CuPt ordering

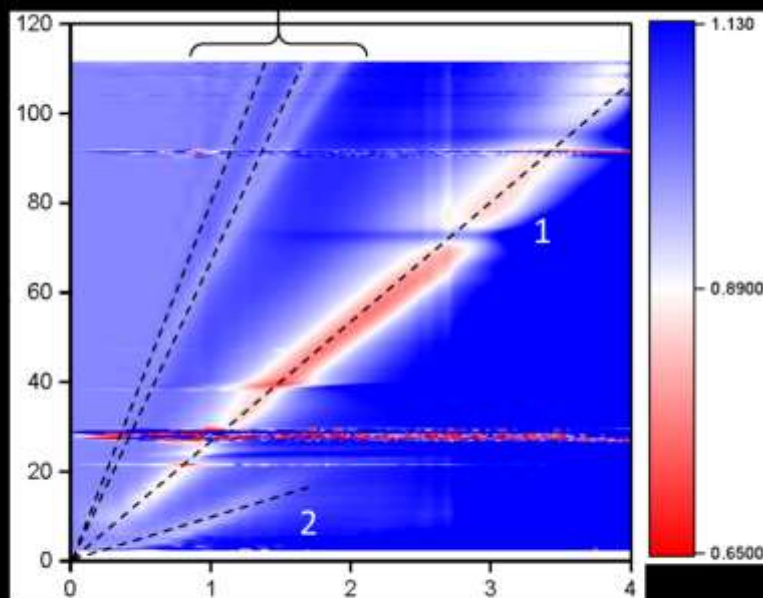


SLS ordering

Measured in ARL

Magneto-absorption of SLS grown on metamorphic buffers

Magnetoabsorption was measured in $\text{InAs}_{0.7}\text{Sb}_{0.3}/\text{InAs}_{0.25}\text{Sb}_{0.75}$ SLS with the effective lattice constant of 6.25 Å, and in $\text{InAs}_{0.48}\text{Sb}_{0.52}/\text{InSb}$ with the effective lattice constant of 6.33 Å.

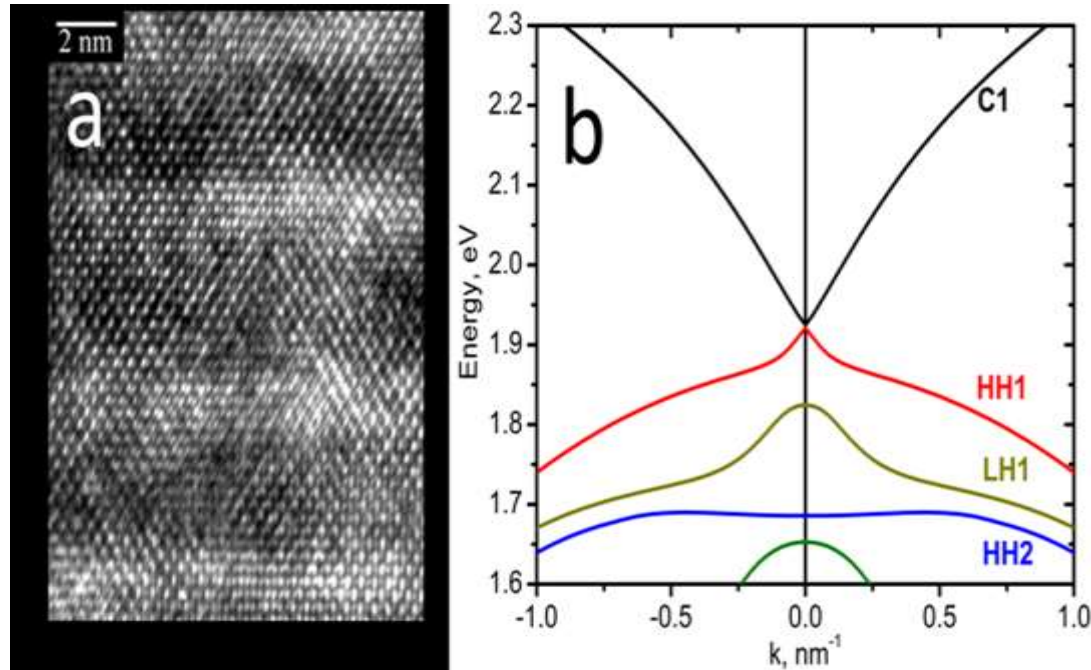


The color plot shows the magnetoabsorption spectra for in $\text{InAs}_{0.48}\text{Sb}_{0.52}/\text{InSb}$ SLS With the period of 6.2 nm.

Line 1 corresponds to the transition between the 0th and 1st electron Landau levels,

Line 2 – to the transition between the 1st and 2nd electron Landau levels. The dashed lines are guides to the eye.

The bandgap, determined as the energy axis intercept of the optical transition energies on a magnetic field is close to zero. The cyclotron energy is proportional to the square root of the magnetic field. This is a direct indication to the linearity of the carrier energy dispersion.



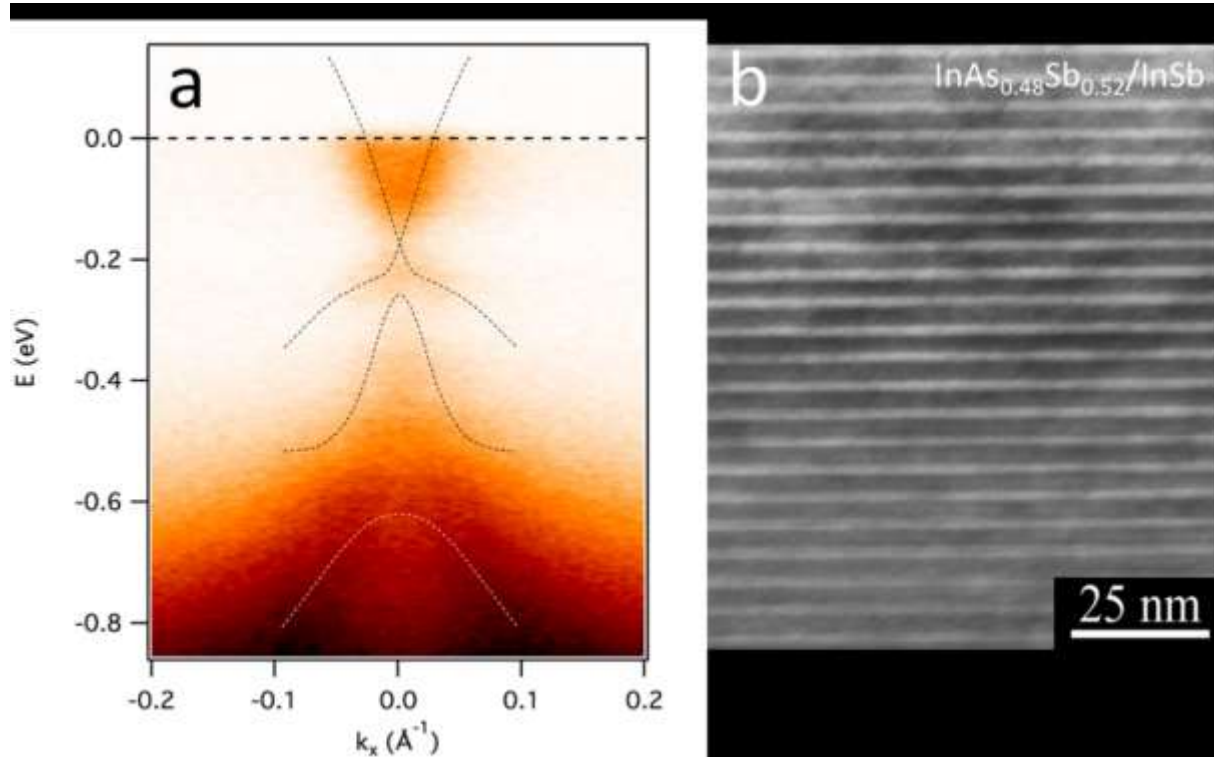
(a) High resolution TEM image of $\text{InAs}_{0.48}\text{Sb}_{0.52}/\text{InSb}$ SLS with the period of 6.2 nm. Clear area corresponds to InSb . Calculated band structure $\text{InSb}/\text{InAsSb}_{0.52}$ SL with a 6.2-nm period. Smooth interfaces with the effective thickness 2nm were used for the model..

(b) Calculation of in-plane and vertical carrier energy dispersion based on NextNano software. The material parameters were obtained from magneto-absorption measurements performed on the bulk InAsSb alloys with various compositions. The model takes into account interface disorder, which is seen on high resolution TEM images (a).



Angle-Resolved Photoemission Spectroscopy

The Dirac-type dispersion was confirmed by the Angle-Resolved Photoemission Spectroscopy (ARPES) data

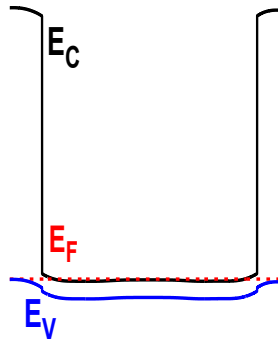


(a) ARPES data of $\text{InAs}_{0.48}\text{Sb}_{0.52}/\text{InSb}$ ordered alloy with the period of 6.2 nm. The dashed lines are 8 band kp calculation.

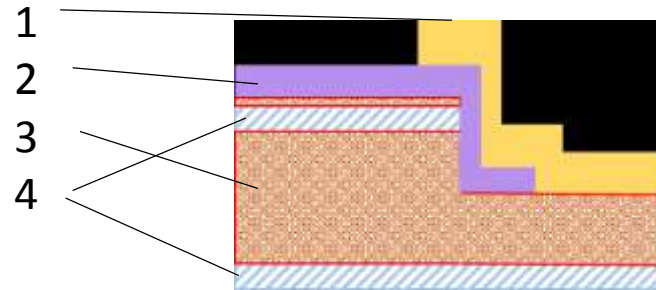
(b) TEM image of same material.

The TEM imaging and transport measurements demonstrate high quality, dislocation-free material which can be used for quantum device applications. Further increase of the ordering period leads to band inversion and opening hybridization gap at the Γ point.

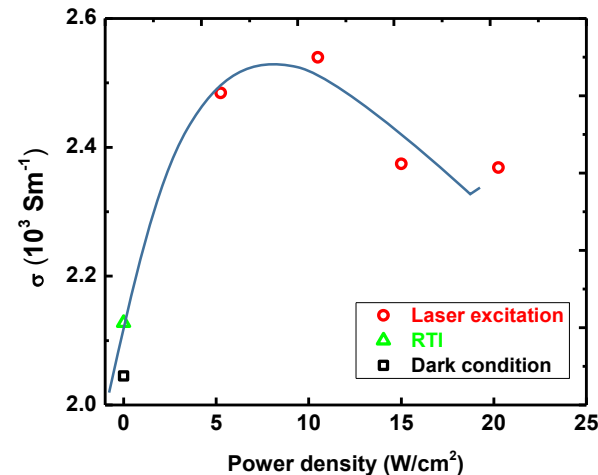
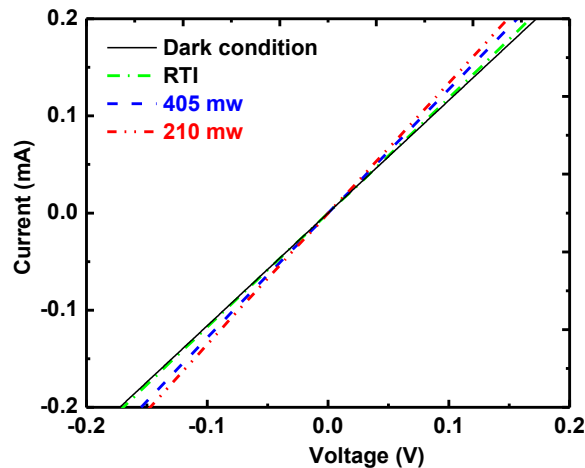
Lateral photoconductivity measurements in a 3.6 nm period InAsSb_{0.6}/InAsSb_{0.3} SLS



The band diagram of the InAsSb_{0.6}/InAsSb_{0.3} SLS absorber. The 1- μm thick SLS absorber was enclosed with low p-doped Al_{0.67}InSb electron confinement layers.



The sample cross-section: 1- metallization, 2- SiN isolation, 3- 1.8 nm/1.8 nm period InAsSb_{0.6}/InAsSb_{0.3} SLS absorber, 4- AllnSb electron confinement layers.

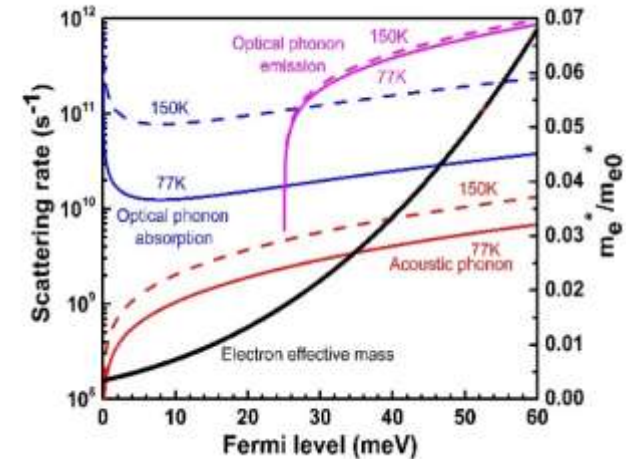


I-V characteristics of the SLS heterostructure and conductivity versus optical power with the bias potential applied along the layers. The heterostructure resistance and conductivity, respectively, showed a non-monotonic dependence on excitation power: the photoconductivity was positive (resistance was decreasing with optical power) under room temperature illumination (RTI) and under a low power excitation with a 10.6 μm CO₂ laser. At higher laser power levels the photoconductivity was decreasing with power. The effect of negative photoconductivity was observed experimentally for the first time.

Modeling of the negative photoconductivity phenomenon in narrow gap semiconductors

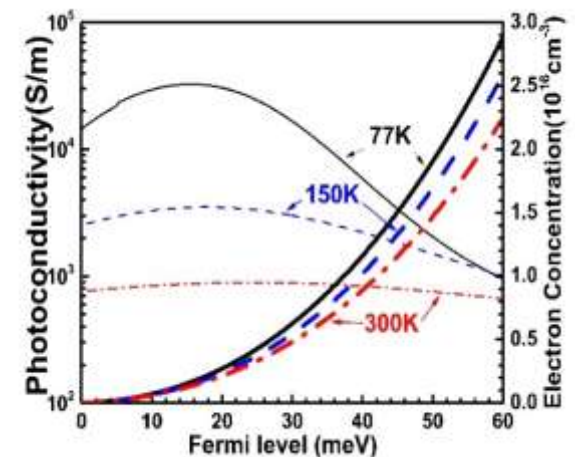
Negative photoconductivity in narrow gap semiconductors is a fundamental phenomenon which occurs in degenerate semiconductors due to fast decrease of electron mobility with increase of excess electron concentration.

The reason for the mobility falling off with quasi-Fermi level is a two fold: (1) due to a rapid decrease of the momentum relation time with energy when the quasi Fermi level approaches the optical phonon energy (24 meV in this case) and (2) due to a rapid increase of the electron effective mass with quasi-Fermi level (black line in the top figure). The electron momentum scattering with optical phonon emission has a threshold at 24 meV (the pink line in the top figure). The bottom figure shows the calculated conductivity and electron concentration versus Fermi level E_f at three temperatures. Note the falling part of the conductivity above $E_f \sim 20$ meV for $T = 77$ and 150 K.

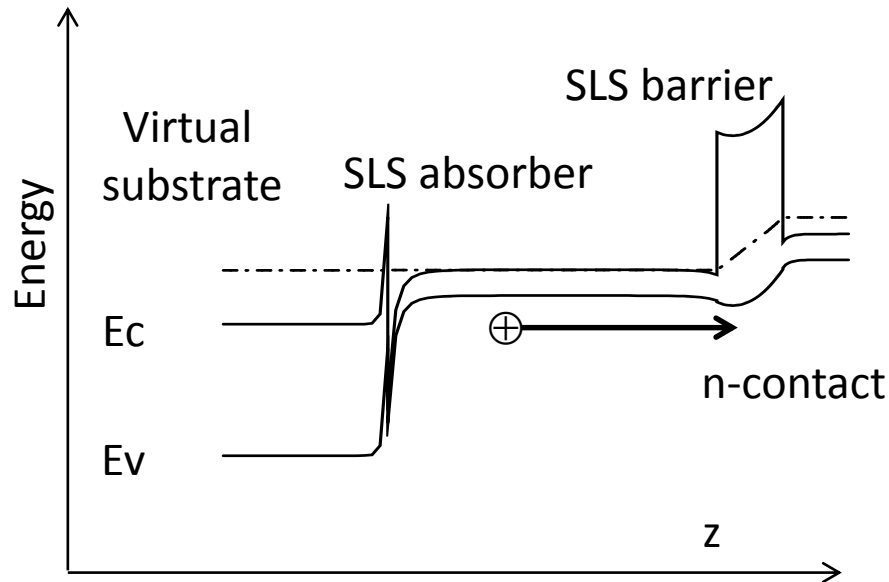


$$\Delta\sigma = \Delta n \cdot e \cdot \mu$$

$$\mu = \frac{e \cdot \tau}{m^*}$$



Barrier heterostructures (nBn design) with short-period SLS absorbers and SLS barriers



The latest design of nBn heterostructure with SLS barrier was obtained without growth interruption at the interface and the contact doping reduced to 10^{17} cm^{-3} . The devices operated with the bias voltage of 0.25 V.

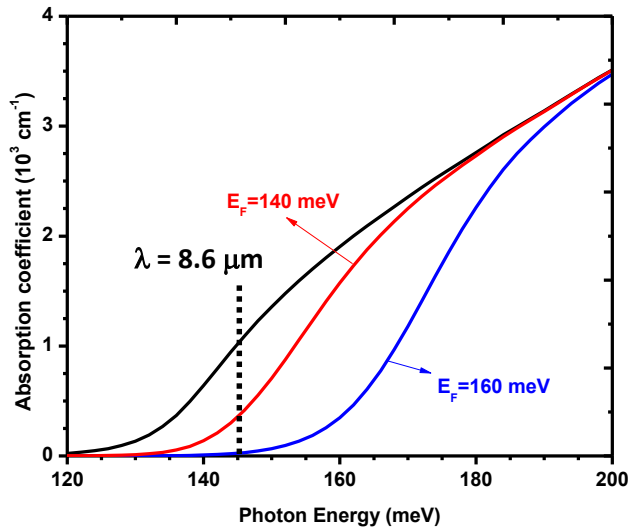
The figure above shows the energy band profile of the barrier heterostructure with a 3.2 nm period $\text{InAsSb}_{0.3}/\text{InAsSb}_{0.6}$ SLS absorber under bias.



Modulation of the optical absorption by carrier injection in nBp heterostructures with bulk InAsSb and short- period SLS



Similar heterostructures have been grown with moderately p-doped barrier and p-contact for study of Auger recombination lifetime and change of the absorption with excess carrier concentration.

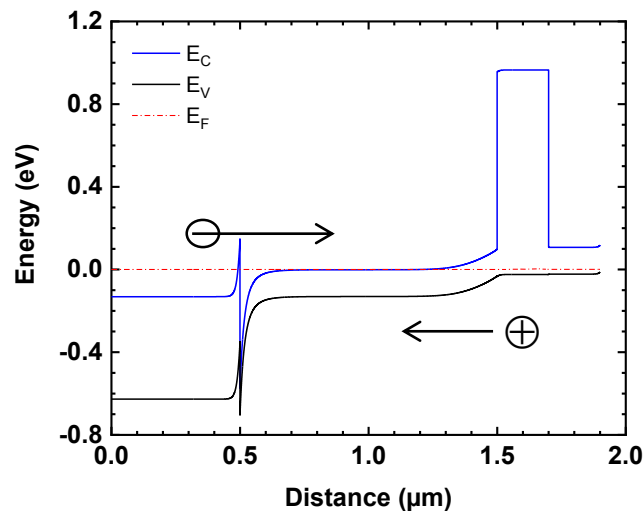


The figure shows the calculated absorption spectra for bulk $\text{InAsSb}_{0.4}$ alloys with the Fermi levels of 130, 140 and 160 meV (black, red and blue lines, respectively). At the photon energy 144 meV ($\lambda = 8.6 \mu\text{m}$) the lift of the Fermi level to 160 meV results in a decrease of the fundamental absorption from 10^3 cm^{-1} to transparency.

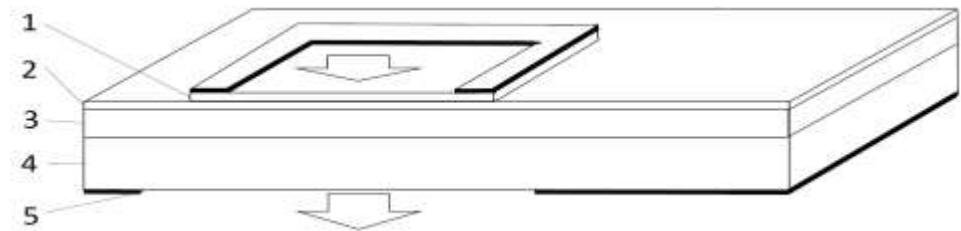
Due to small effective mass ($0.011 m_0$ in bulk $\text{InAsSb}_{0.4}$) and small density of states at $T = 77 \text{ K}$, respectively, at $\lambda = 8.6 \mu\text{m}$ the transparency occurs at electron concentration level of 10^{16} cm^{-3} . The latter implies Auger limited injection current densities of $10\text{-}20 \text{ A/cm}^2$.

With $1\text{-}\mu\text{m}$ thick pilot structures with bulk $\text{InAsSb}_{0.4}$ and 3.2 nm period SLS absorbers the modulation depths of 9 % and 7 % were demonstrated under pulsed current injection at the wavelengths of 8.6 and $10.6 \mu\text{m}$, respectively.

Free-space optical beam intensity modulation with bulk $\text{InAsSb}_{0.4}$ heterostructures



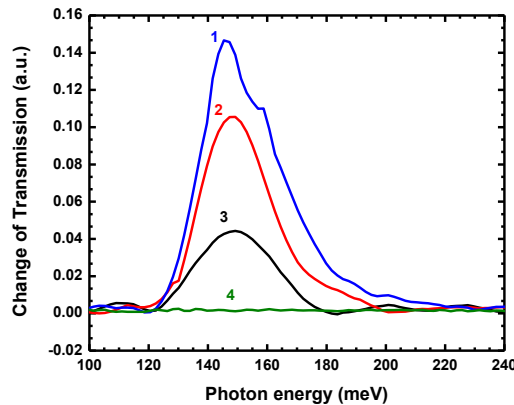
(a)



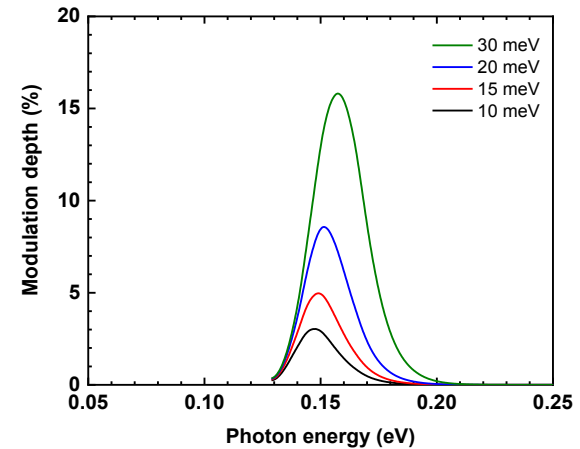
(b)

- (a) The energy band diagram of the heterostructure with the bulk InAsSb absorber in equilibrium: E_F , E_C , E_V are the Fermi level and conduction and valence band edges.
- (b) Schematic cross-section of the heterostructure consisting of a 1 μm thick $\text{InAsSb}_{0.4}$ absorber: 1- mesa contact with the front ring metal and a window for the incident light, 2- electron barrier layer, 3- absorber, 4- substrate, 5- the backside metal with a window for the transmitted light.

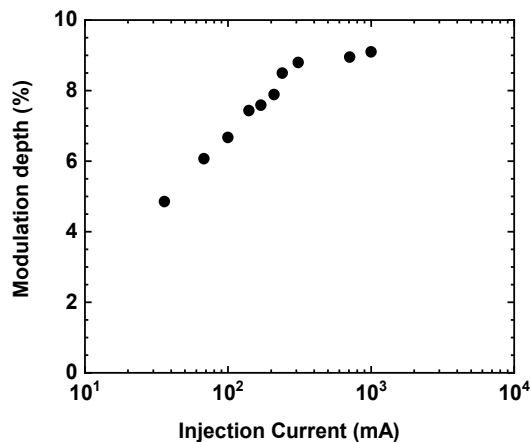
Free optical beam intensity modulation with bulk $\text{InAsSb}_{0.4}$ heterostructures



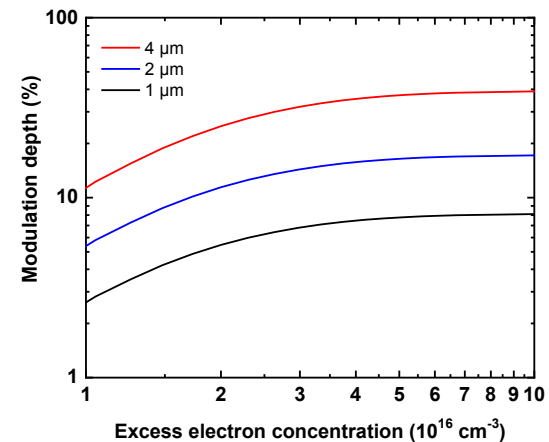
The modulation spectra of a heterostructure at $T = 77$ K with a 1 μs pulse width and a 100 kHz repetition rate for the injection currents of 20, 100, and 500 mA.



The calculated modulation spectra of a 1- μm -thick InAsSb absorber with $E_g = 133$ meV at $T = 77$ K for electron quasi-Fermi levels of $E_F = 10, 15, 20,$ and 30 meV above the bottom of the conduction band E_C

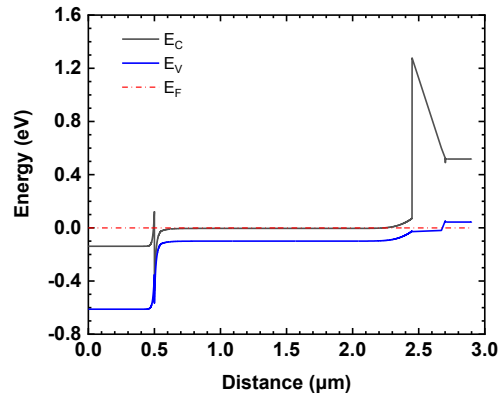


The modulation depth vs injection current with a 100 ns pulse width and a 10 kHz repetition rate in the heterostructure illuminated with a continuous wave QCL, $\lambda = 8.6$ μm .

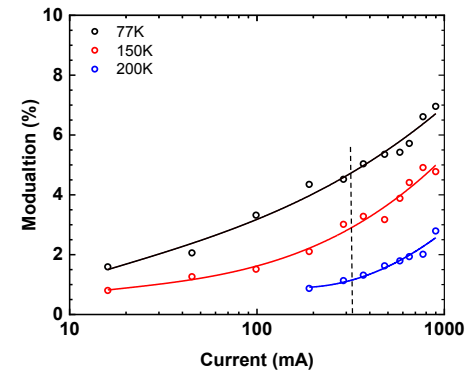


The calculated modulation depth at a laser photon energy of 144 meV ($\lambda = 8.6$ μm) vs excess carrier concentration for the absorber thicknesses $W = 1, 2,$ and 4 μm

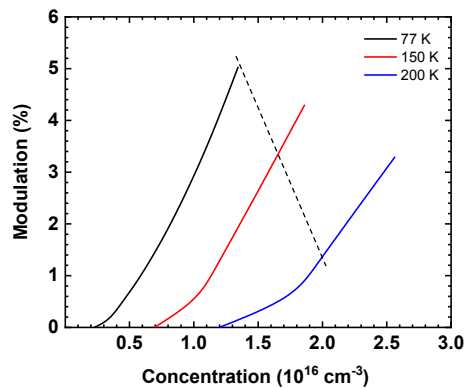
Free-space optical beam intensity modulation with $\text{InAsSb}_x/\text{InAsSb}_y$ SLS heterostructures



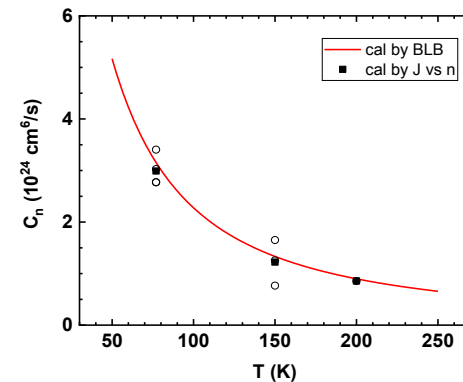
The band diagram of the nBp heterostructure with a 85 meV energy gap SLS absorber consisting of a 3.45 nm period SLS $\text{InAsSb}_{0.66}/\text{InAsSb}_{0.35}$



Modulation depth of the heterostructures with injection current measured at $\lambda = 10.6 \mu\text{m}$ in the temperature range from 77 to 200 K. The dashed line shows that at the injection current of 330 mA at the temperatures of 77, 150 and 200 K the modulation depths of about 5, 3 and 1 %, were observed

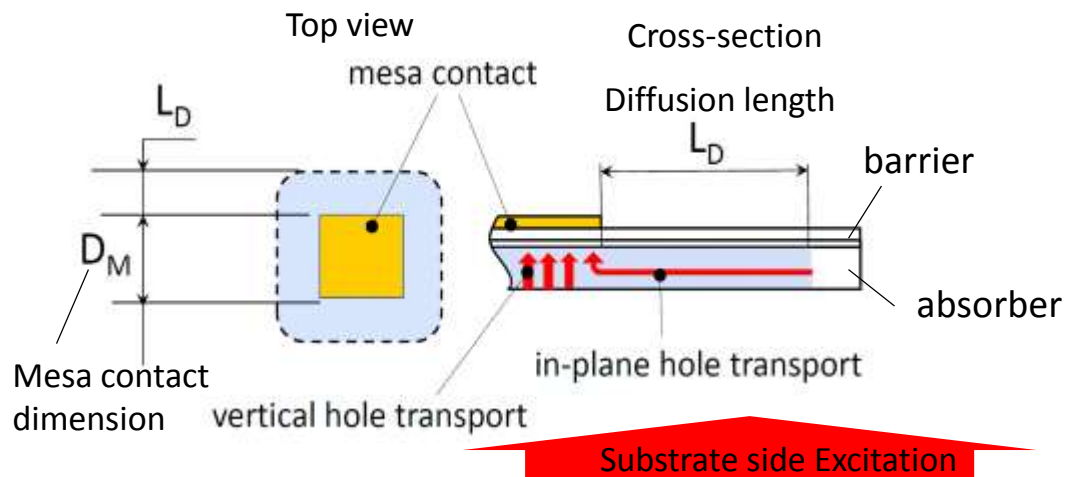


Calculated dependences of the modulation depth versus carrier concentration. The dashed line drawn through the modulation depth points of 5, 3 and 1 % for the dependences for $T = 77, 150$ and 200 K illustrates that for a given injection current the excess carrier concentration was increasing with temperature.



Temperature dependence of Auger coefficient extracted with modulation data vs injection current and the Beattie-Landsberg-Blakemore (BLB) fit.

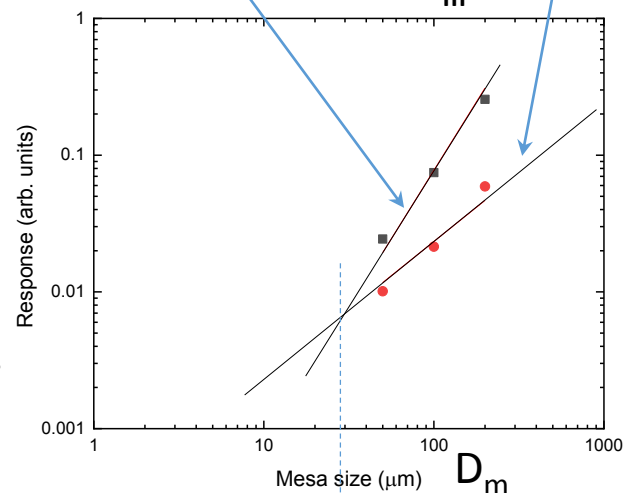
Minority hole lifetime and in-plane hole diffusion length in short-period InAsSbx/InAsSby SLS grown on metamorphic buffers



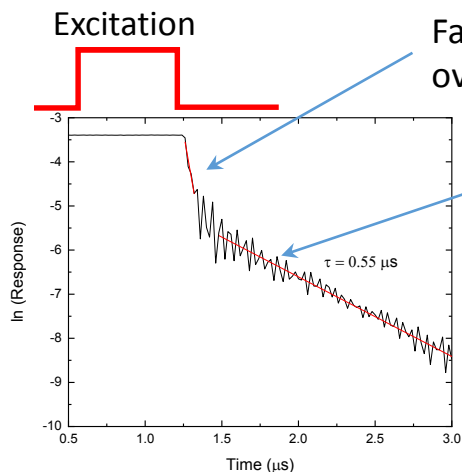
Measuring photocurrent in structures with variable mesa width D_M makes it possible to determine diffusion length L_D .

Amplitude of the fast part of the response decay is proportional to area D_m^2

Amplitude of long decay is linear with D_m



$$\text{Response} = J_{\text{vertical}} \times D_M^2 + J_{\text{in_plane}} \times 4 D_M L_D$$



Hole lifetime = $0.55 \mu\text{s}$
Lateral hole diffusion length = $7.5 \mu\text{m}$

Parameters of bulk $\text{InAsSb}_{0.4}$ alloys at $T = 77 \text{ K}$

Energy gap (eV)	Electron effective mass (m_0)	Electron mobility (cm^2/Vs)	Hole mobility (cm^2/Vs)	Hole diffusion length (μm)
0.12 eV	0.011	179,000	1000	9

Energy gap and minority hole lifetime at $T = 77 \text{ K}$

Parameters	bulk InAsSb Sb =40 %	InAsSb _x / InAsSb _y SLS	
		4.3 nm	2.3 nm
Energy gap (eV)	0.12	0.12	0.08
Minority hole lifetime (ns)	185	550	140

The material parameters were measured by direct methods. The minority hole lifetime values in materials obtained with metamorphic GaInSb buffers are similar to those reported for materials obtained with pseudomorphic growth on GaSb.

Summary

- 1. The developed novel approach to growth on metamorphic buffers allowed to obtain quality bulk and SLS InAsSb-based semiconductor compounds with energy gaps < 0.1 eV to cover entire LWIR wavelength range and compounds with inverted energy bands.**
- 2. Enabling the lattice constant as a design parameter opens windows of other parameters for optimization and considerable improvement of the performance of infrared photonic devices based on III-V compound barrier heterostructures.**
- 3. A factor of 3 stronger fundamental absorption, unimpeded vertical hole transport and microsecond scale hole lifetime at 77 K have been demonstrated for Ga-free SLS grown on metamorphic buffers.**
The improved parameters can be traded for increasing device operating temperature.